

Functional Assembly of Aptamer Binding Sites by Single-Molecule Cut-and-Paste

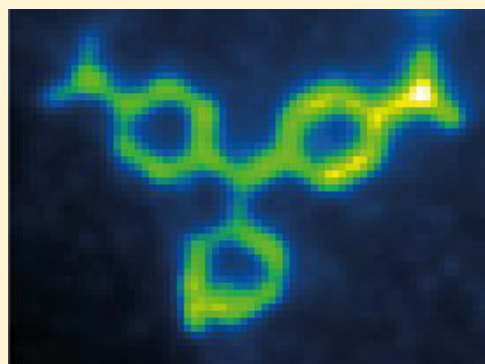
Mathias Strackharn,[†] Stefan W. Stahl,[‡] Elias M. Puchner,[§] and Hermann E. Gaub^{*,†}

[†]Center for Nanoscience and Department of Physics, University of Munich, Amalienstraße 54, 80799 Munich, Germany

[‡]Center for Integrated Protein Science (CIPSM), Munich, Germany

Supporting Information

ABSTRACT: Bottom up assembly of functional molecular ensembles with novel properties emerging from composition and arrangement of its constituents is a prime goal of nanotechnology. By single-molecule cut-and-paste we assembled binding sites for malachite green in a molecule-by-molecule assembly process from the two halves of a split aptamer. We show that only a perfectly joined binding site immobilizes the fluorophore and enhances the fluorescence quantum yield by several orders of magnitude. To corroborate the robustness of this approach we produced a micrometer-sized structure consisting of more than 500 reconstituted binding sites. To the best of our knowledge, this is the first demonstration of one by one bottom up functional biomolecular assembly.



KEYWORDS: Functional assembly, RNA aptamer, single-molecule cut-and-paste, single-molecule fluorescence, single-molecule force spectroscopy, atomic force microscope (AFM)

Feynman is frequently quoted for having foreseen that individual atoms may be arranged one by one to form functional assemblies, moreover that covalent reactions between them may then provide a unique way to synthesize new molecules atom by atom.¹ The seminal work by Eigler and colleagues^{2,3} convincingly proved the validity of these concepts: functional assemblies of atoms forming quantum corrals showed emergent novel properties. The application of these strategies to biomolecules, however, turned out to be much more challenging. A quite vivid dispute was fought in a series of papers between Smalley and Drexler on where these difficulties arise and whether fundamental limitations prevent the molecule for molecule assembly of biomolecules in electrolyte ambient at physiologic temperatures.⁴ Hans Kuhn had realized early on that for many multistep biological reactions not only the sequence but also the arrangement of the individual enzymes plays a crucial role. He envisaged that in order to investigate their interaction, novel approaches would be needed; he wished to have molecular pliers to pick up and place individual enzymes to create functional assemblies with designed properties.⁵

With the development of single-molecule cut-and-paste (SMC&P), we provided a platform technology for the assembly of biomolecules at surfaces.⁶ It combines the Å-positioning precision of the AFM^{7,8} with the selectivity of DNA hybridization to pick up individual molecules from a depot area and arrange them at a construction site one by one.⁹ We localized the pasted molecules with nanometer accuracy by single molecule fluorescence and showed that the deposition

accuracy is presently limited by the length of the spacers used to couple the DNA handles and anchors to the tip and construction site, respectively.¹⁰ We assembled structures with dimensions below the Abbé diffraction limit and imaged them by superresolution Blink-microscopy.¹¹ We thoroughly validated SMC&P and proved it to be a robust technology with the potential of high throughput. In this paper, we take the next important step and demonstrate the functional assembly of a biomolecular complex with a novel emergent property from individual building blocks one by one at a chosen position on a surface (see Figure 1).

Malachite green (MG) is a well-established red-emitting fluorophore whose quantum yield is known to depend strongly on the rotational degrees of freedom of its phenyl rings.^{12,13} An increase in the quantum yield up to several orders of magnitude upon binding of this molecule to either BSA films,¹⁴ specific antibody binding pockets¹⁵ or suitable RNA structures^{16,17} was reported in the literature. Particularly interesting appears the work by Kolpashchikov¹⁸ where it was shown that a MG-aptamer may be split in two and used as DNA sensors with single mismatch resolution. Neither of the two aptamer halves was reported to improve the quantum yield of MG significantly, but both halves combined form a complete binding pocket and enhance the MG fluorescence by more than 3 orders of magnitude (cf. Supporting Information).

Received: February 1, 2012

Revised: March 28, 2012

Published: April 3, 2012

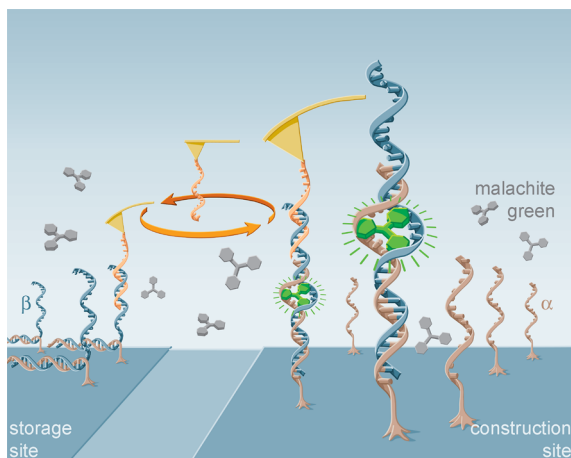


Figure 1. Schematics of the assembly of functional binding sites produced by SMC&P from individual α - and β -chains of a split malachite green aptamer. At the construction site, α -chains were covalently anchored at the 3' end via PEG-spacers. At the storage site, β -chains were hybridized with a 40 bp overlap to an anchor oligo, which was covalently bound via its 5' end to the surface. The other end of the β -strand had been extended by a 20 bases handle sequence, compatible to the corresponding handle oligo at the AFM cantilever tip. For transport, this handle oligo was brought into contact with a β -strand, allowing the two strands to hybridize. Upon retraction of the cantilever, the anchor oligo in unzip geometry yields and the β -strand is moved to the construction site, where it is positioned such that it hybridizes with an α -strand to form a complete MG binding site. Upon retraction of the tip, the handle sequence in shear geometry yields and the tip is free to pick up the next β -strand. When malachite green is bound in the fully assembled aptamer, its quantum yield is increased by more than 3 orders of magnitude, resulting in a bright fluorescence of the complex.

In order to directly compare the emission of individual MG aptamer complexes consisting of one α - and one β -strand each to that of Cy5 molecules under identical excitation and detection conditions, we covalently bound a very dilute layer ($<1/5 \mu\text{m}^2$) of β -strands with a thiol group at the 3' end to a glass surface and then hybridized them with α -strands carrying one Cy5 label at the 3' end. We identified individual Cy5 molecules by TIRF microscopy¹⁹ and localized them by fitting Gauss functions to the intensity distributions. Once the Cy5 molecules were irreversibly photobleached (Figure 2 trace a) we added a 50 nM solution of MG and recorded the emission again. Now an intermittent signal was recorded. The fluorescent MG molecules were also localized to ensure that fluorescence from Cy5 and MG were colocalized (cf. Supporting Information). Trace b in Figure 2 shows a typical example of the intermittent emission pattern that we measured for extended periods of time up to several minutes. Note that the baseline of the MG emission is within an error bar of 10% indistinguishable from that of the bleached Cy5, which means that at the given concentration the free MG in solution does not significantly contribute to the measured fluorescence. It is not clear yet whether this pulsing fluorescence is caused by a change in the electronic structure of MG (e.g., population of triplet states) or by conformational changes in the molecular MG-aptamer complex (e.g., binding/unbinding of MG). It may as well reflect slow modes of the hybridization dynamics of the aptamer binding pocket. MG in the aptamer binding pocket might also become photobleached and replaced by intact MG

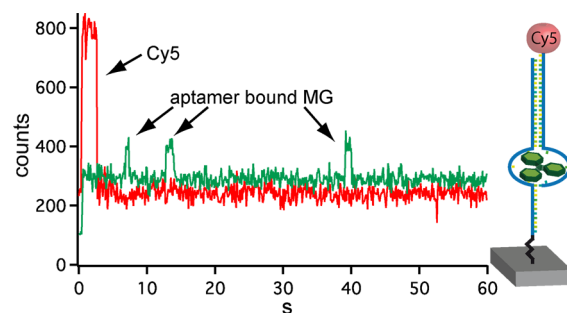


Figure 2. Typical fluorescence emission traces of individual molecules. In red, the emission of an individual Cy5 label at the 3' end of an α -strand of the split MG-aptamer. After several seconds, the Cy5 is photobleached irreversibly and the emission drops to the background level. We then added 50 nM malachite green to the buffer solution and recorded the emission from the same aptamer under otherwise identical conditions (green trace). We measured a slightly increased background level and an intermittent fluorescence pattern with pulse durations of typically 3 ± 1 s. The typical height of the pulses was only one-fifth of the Cy5 emission. The insert depicts the molecular construct.

during these traces. Detailed future studies will be required to further elucidate these interesting phenomena.

Having verified that hybridization of the aptamer leads to a marked increase in the MG fluorescence at the surface, we assembled $\alpha\beta$ -aptamer arrangements by SMC&P. We modified the split aptamers such that we were able to handle and reassemble them one by one to form fully functional MG binding sites. We used different areas on a cover glass for storage and construction sites (see Figure 1) and used a functionalized AFM tip to pick up individual β -aptamer strands from the depot side and to paste them in the construction site at a given position. Since the AFM tip is then ready again to pick up a β -aptamer strand, SMC&P can be operated as a cyclic process.

All experiments were carried out with a custom built AFM/TIRF hybrid microscope²⁰ as follows: In the presence of 50 nM MG in solution first the background image from the still empty construction site was recorded. Then the AFM tip was traversed toward the storage area and lowered toward the surface, while a force distance trace was recorded. The functionalization densities on the tip and the storage surface were chosen such that in approximately every third approach the handle oligos on the tip and a β -strand of the aptamer hybridized, resulting in a specific molecular multisegment chain between tip and surface. Upon retraction, the force is gradually built up in this chain, and the weakest of the segments yields (see Figure 3a). Note that the attachment geometries were chosen such that the handle oligos are loaded in shear geometry, which means that the hydrogen bonds are all loaded roughly equally, whereas the anchor is loaded in unzip geometry, which means that base pair for base pair sequentially unbinds. As a result, with a 95% likelihood it is the anchor that yields while the β -strand of the aptamer remains bound to the tip via its 20 bp handle. Despite the higher hybridization energy between the β -strand of the aptamer and the anchor oligo compared to the handle oligos, the force to open the hybrid in unzip geometry is much lower than the force required to open the hybrid in shear geometry because the mechanical work to separate the two halves is performed over a much larger distance than in the first case. Typical examples of the force distance traces recorded during the cut process are shown in

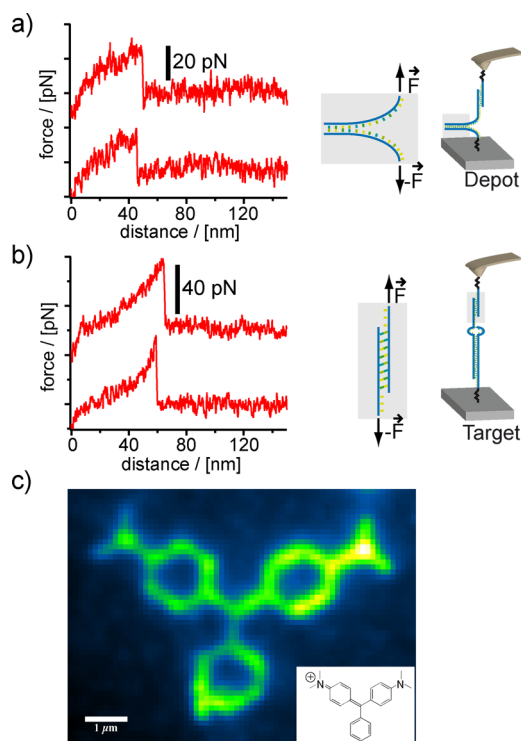


Figure 3. Typical force distance protocols of the cut (a) and paste (b) processes highlighted in Figure 1. (c) Fluorescence micrograph of a structure, consisting of more than 500 aptamers, which were assembled by SMC&P with the same tip. The insert shows the structural formula of MG that served as a blueprint of the arrangement.

Figure 3a. The rising parts of the curves reflect the entropic elasticity of the polymeric anchors, and the short plateau before the force drops to zero is caused by the unzipping of the DNA.

With the force distance curve corroborating that exactly one β -aptamer strand was picked up (see Figure 3a), the AFM tip was traversed to the construction side and lowered at a chosen position.²¹ If the two halves of the split aptamer hybridize, again a chain is formed that is loaded when the tip is retracted from the surface. Since the two halves of the aptamer have a much longer sequence overlap than the handle oligos, the handle oligo complex yields (again with >90% probability) after which the tip is free to pick up a new molecule in the next cycle. Since again a force distance curve (see Figure 3b) was recorded, the deposition was either corroborated or a further attempt to paste the molecule was undertaken. Upon separation, the force distance traces depicted in Figure 3b show a continuous increase in force until the two strands loaded in shear geometry suddenly split in an all or none event and the force drops to zero.

In previous studies, we had shown that we can localize individual molecules by super resolution microscopy with an accuracy of better than 2 nm, and that the precision of the paste process is better than 10 nm. In this study here, we focused on the robustness of the process and repeated the cycle described above more than 500 times to assemble the pattern shown in Figure 3c. It depicts to the best of our knowledge the first example of a structure in which biomolecules were assembled one by one in a physiological ambient to perform a function, which emerges exclusively from their correct assembly. The bright fluorescence unambiguously corroborates that we have

assembled functional binding sites from the two halves of the aptamer, and the well-pronounced contrast shows that we did so with superb selectivity.

This proof of principle opens the door toward the assembly of increasingly complex multicomponent systems at surfaces. Since we have already demonstrated that proteins or nanoparticles may be arranged by SMC&P, a large variety of systems with diverse molecular functions, which emerge from the unique arrangement of the constituents, may be envisioned. In combination with recent developments for the rapid production of protein libraries on microfluidic chips,²² SMC&P will promote design and assembly of functional protein arrays or even entangled enzymatic networks.

■ ASSOCIATED CONTENT

Supporting Information

Details of material and methods, sample preparation, AFM measurements, TIRF-microscopy, fluorescence properties of the aptamer bound MG; additional results from nanometer precise localization and colocalization of Cy5 label and MG fluorescence. This material is available free of charge via the Internet at <http://pubs.acs.org>.

■ AUTHOR INFORMATION

Corresponding Author

*E-mail: gaub@lmu.de. Fax: +49 89 2180 2050.

Present Address

[§]Department of Cellular and Molecular Pharmacology, University of California, San Francisco, CA.

Notes

The authors declare no competing financial interest.

■ ACKNOWLEDGMENTS

This work was supported by the German Science Foundation and the Nanosystems Initiative Munich. Fruitful discussions with Ralf Jungman, Philip Severin, and Philip Tinnefeld are gratefully acknowledged.

■ REFERENCES

- (1) Feynman, R. P. *Eng. Sci.* **1960**, *23* (5), 22–36.
- (2) Crommie, M. F.; Lutz, C. P.; Eigler, D. M. *Science* **1993**, *262* (5131), 218–220.
- (3) Jung, T. A.; Schlittler, R. R.; Gimzewski, J. K.; Tang, H.; Joachim, C. *Science* **1996**, *271* (5246), 181–184.
- (4) Baum, R. *Chem. Eng. News* **2003**, *81* (48), 37–42.
- (5) Kuhn, H. *Verh. Schweiz. Naturforsch. Ges.* **1965**, 245–266.
- (6) Kufer, S. K.; Puchner, E. M.; Gump, H.; Liedl, T.; Gaub, H. E. *Science* **2008**, *319* (5863), 594–596.
- (7) Binnig, G.; Quate, C. F.; Gerber, C. *Phys. Rev. Lett.* **1986**, *56* (9), 930–933.
- (8) Drake, B.; Prater, C. B.; Weisenhorn, A. L.; Gould, S. A. C.; Albrecht, T. R.; Quate, C. F.; Cannell, D. S.; Hansma, H. G.; Hansma, P. K. *Science* **1989**, *243* (4898), 1586–1589.
- (9) Puchner, E. M.; Kufer, S. K.; Strackharn, M.; Stahl, S. W.; Gaub, H. E. *Nano Lett.* **2008**, *8* (11), 3692–3695.
- (10) Kufer, S. K.; Strackharn, M.; Stahl, S. W.; Gump, H.; Puchner, E. M.; Gaub, H. E. *Nat. Nanotechnol.* **2009**, *4* (1), 45–49.
- (11) Cordes, T.; Strackharn, M.; Stahl, S. W.; Summerer, W.; Steinhauer, C.; Forthmann, C.; Puchner, E. M.; Vogelsang, J.; Gaub, H. E.; Tinnefeld, P. *Nano Lett.* **2010**, *10* (2), 645–651.
- (12) Ben-Amotz, D.; Harris, C. B. *Chem. Phys. Lett.* **1985**, *119* (4), 305–311.
- (13) Abedin, K. M.; Ye, J. Y.; Inouye, H.; Hattori, T.; Sumi, H.; Nakatsuka, H. *J. Chem. Phys.* **1995**, *103* (15), 6414.

- (14) Bartlett, J. A.; Indig, G. L. *Dyes Pigm.* **1999**, *43* (3), 219–226.
- (15) Szent-Gyorgyi, C.; Schmidt, B. F.; Creeger, Y.; Fisher, G. W.; Zakel, K. L.; Adler, S.; Fitzpatrick, J. A.; Woolford, C. A.; Yan, Q.; Vasilev, K. V.; Berget, P. B.; Bruchez, M. P.; Jarvik, J. W.; Waggoner, A. *Nat. Biotechnol.* **2008**, *26* (2), 235–240.
- (16) Babendure, J. R.; Adams, S. R.; Tsien, R. Y. *J. Am. Chem. Soc.* **2003**, *125* (48), 14716–14717.
- (17) Grate, D.; Wilson, C. *Proc. Natl. Acad. Sci. U.S.A.* **1999**, *96* (11), 6131–6136.
- (18) Kolpashchikov, D. M. *J. Am. Chem. Soc.* **2005**, *127* (36), 12442–12443.
- (19) Tokunaga, M.; Kitamura, K.; Saito, K.; Iwane, A. H.; Yanagida, T. *Biochem. Biophys. Res. Commun.* **1997**, *235* (1), 47–53.
- (20) Gumpp, H.; Stahl, S. W.; Strackharn, M.; Puchner, E. M.; Gaub, H. E. *Rev. Sci. Instrum.* **2009**, *80* (6), 063704.
- (21) If the force curve indicates that the pick up was not successful, the online control of the process allows for another pick-up attempt. If the force curve indicates that several molecules were picked up, they can be pasted in a “wastebasket” area rendering the tip ready again for the normal cycle.
- (22) Gerber, D.; Maerkl, S. J.; Quake, S. R. *Nat. Methods* **2009**, *6* (1), 71–74.

Supporting Information

Functional Assembly of Aptamer Binding Sites

by Single-Molecule Cut-and-Paste

Mathias Strackharn¹, Stefan W. Stahl^{1,2}, Elias M. Puchner^{1,3} & Hermann E. Gaub^{1,*}

¹ Center for Nanoscience and Department of Physics, University of Munich, Amalienstraße 54, 80799 Munich, Germany

² Center for Integrated Protein Science (CIPSM), Munich, Germany

³ The author has moved to the Department of Cellular and Molecular Pharmacology, University of California, San Francisco, 600 16th Street, San Francisco, CA 94158, USA

* gaub@lmu.de

All measurements described in the manuscript were carried out with a custom designed combined AFM/TIRF microscope described in detail in ¹. Here the description of those parts and procedures, which are relevant to the experiments described above:

AFM Measurements

The spring constants of the DNA modified cantilevers were calibrated in solution using the equipartition theorem ^{2,3}. For the single-molecule force-extension trace recordings BL-AC40TS cantilevers (Olympus Cooperation, Tokyo, Japan) were used with a typical spring constant of about 120 pN/nm and a resonance frequency of 30 kHz. This experiment was conducted in 100 mM sodium phosphate buffer, pH 5.5, 140 mM NaCl, 5 mM MgCl₂. For the functional assembly of the Malachite Green structure pattern MLCT-AUHW levers (Bruker, Camarillo, USA) were used. The protocol for the functional assembly as well as the data recording was programmed using Igor Pro (Wave Metrics) and an Asylum Research MFP3D controller, which provides ACD and DAC channels as well as a DSP board for setting up feedback loops. Cantilever positioning for pick-up and delivery was controlled in closed-loop operation. The typical cycle time for one functional assembly process lies between 2 and 3 seconds depending on the sample orientation and the traveling distance between depot and target area. The positioning feedback accuracy is ± 3 nm however long term deviations may arise due to thermal drift. Extension velocities are set between 1 and 2.5 $\mu\text{m/s}$.

Measurements with TIRF microscopy

The fluorescence microscopy measurements were carried out with objective-type TIRF excitation on a microscope that was especially designed for a stable combination of AFM with TIRFM¹. We excited with a fiber-coupled 639 nm diode laser (iBeam smart, TOPTICA, München, Germany) through a 100x/1.49 oil immersion objective lens (Nikon CFI Apochromat TIRF, Japan). As excitation filter, beam splitter, and emission filter a BrightLine HC 615/45, a Raman RazorEdge 633 RS, and a Chroma ET 685/70 (AHF, Tübingen, Germany) were used respectively. Images were taken with a back-illuminated EMCCD camera (DU-860D, Andor, Belfast, Ireland). After the functional assembly of the Malachite Green structure pattern 1 μ M Malachite Green (Sigma, Taufkirchen, Germany) in PBS was added. For the single-aptamer fluorescence experiment single aptamers were identified by the fluorescence of the Cy5 label and its single-step bleaching. 100 nM Malachite Green in 100 mM sodium phosphate buffer, pH 5.5, 140 mM NaCl, 5 mM MgCl₂, was added. Fluorescence image sequences were taken at 10 Hz frame rate, gain 200, 1 MHz readout rate in frame transfer mode. The camera was operated at -80 °C.

Preparation of cantilevers

Cantilevers (MLCT, Bruker, Camarillo, USA, and Olympus AC40TS, Japan) were oxidized in a UV-ozone Cleaner (UVOH 150 LAB, FHR Anlagenbau GmbH, Ottendorf-Okrilla, Germany) and silanized with 3-aminopropyltrimethoxysilane (ABCR, Karlsruhe, Germany), baked at 80 °C, pre-incubated with sodium borate buffer (pH 8.5), PEGylated with NHS-PEG-Maleimide (MW 5000, Rapp Polymere, Tübingen, Germany), and washed with ddH₂O as described in⁴.

Thiolated cantilever DNA oligomers were reduced with 5 mM TCEP (Thermo Fisher Scientific, Rockford, USA) for 1 h at room temperature, purified by ethanol precipitation and dissolved again in a 50 mM sodium phosphate buffer, pH 7.2, 50 mM NaCl, 10 mM EDTA to a final concentration of 10 μ M. The PEGylated cantilevers were then incubated at room temperature with the cantilever DNA oligomers for 1 h and rinsed with ddH₂O.

Preparation of cover glass surfaces

Cover glass slips were sonicated in 50% (v/v) 2-propanol and ddH₂O for 15 min and thoroughly rinsed with ddH₂O. They were then oxidized in 50% (v/v) sulfuric acid and hydrogen peroxide (30%) for 45 min and were then again well rinsed with ddH₂O. In addition a UV-ozone treatment was applied for 15 min. For the assembly of the Malachite Green structure pattern the cover glass slips were incubated overnight with 10 mg/ml amino dextran (MW 500000, Invitrogen, Carlsbad, USA), washed afterwards with ddH₂O and dried with a nitrogen stream. NHS-PEG-maleimide (MW 5000) was dissolved to 10 mM in a 50 mM sodium borate buffer, pH 8.5 and incubated on the cover glasses for 1 h. Cover glasses were then washed with ddH₂O. A microfluidic system was fixed on the cover glass. Thiolated depot DNA oligomers and target hybrid oligomers (IBA, Göttingen, Germany) were each reduced with 5 mM TCEP (Thermo Fisher Scientific, Rockford, USA) for 1 h at room temperature, purified by ethanol precipitation and dissolved again in a 50 mM sodium phosphate buffer, pH 7.2, 50 mM NaCl, 10 mM EDTA to a final concentration of 10 μ M. The depot oligomers and the target hybrid oligomers were pumped through the respective channel of the microfluidics for 1 h. Both channels were then rinsed with ddH₂O. A solution 1 μ M transfer hybrid oligomers and 5 nM Atto647N labelled

transfer oligomer in PBS were pumped through the depot channel for 30 min. We used this minor fraction of fluorescent labelled DNA to allow for an exact alignment of the sample with the AFM cantilever. The channel was then rinsed with PBS to remove non-hybridized transfer hybrids. The microfluidic system was then removed again.

For force spectroscopy of the transfer process, the oxidized cover glass slips were silanized with a mixture of 2% 3-aminopropyltrimethoxysilane, 90% EtOH, 8% ddH₂O for 1 h. Cover glasses were thoroughly rinsed with pure EtOH first and ddH₂O afterwards, and were baked at 80 °C for 30 min. After 30 min soaking in 50 mM sodium borate buffer, pH 8.5 the cover glasses were treated with 50 mM NHS-PEG-maleimide (MW 5000) in the sodium borate buffer for 1h and then rinsed with ddH₂O. As for the Malachite Green structure writing experiment, the depot oligomers and the target hybrid oligomers were reduced, purified and dissolved again. The reduced depot and target hybrid oligomers were deposited with a 30 µm capillary of a microplotter (GIX, Sonoplot, Middleton, USA) in two 800 µm long lines separated by around 30 µm. Molecules in solution were flushed away with ddH₂O and a line with 1 µM transfer hybrid oligomers and 5 nM of Atto647N labeled transfer oligomer in 4xPBS was plotted on top of the depot line. Non-hybridized oligomers were flushed away with 4xPBS.

For fluorescence spectroscopy experiments of single aptamers, the oxidized cover glass slips were functionalized with 10 mg/ml NHS-PEG-maleimide (MW 5000) in 50 mM sodium borate buffer, pH 8.5 for 1 h and then rinsed with ddH₂O. Thiolated transfer hybrid oligomers were reduced, purified and dissolved in the same fashion as described before. The cover glass slips were incubated with the reduced thiolated transfer hybrid for 1h, the sample was then washed with ddH₂O. Cover glasses were mounted on the fluorescence microscope and Cy5 labelled target

hybrid oligomers were hybridized in a 100 mM phosphate buffer, pH 5.5, 140 mM NaCl, 5 mM MgCl₂ to the surface bound transfer hybrid oligomers. The density was chosen such that it allowed for single molecule fluorescence spectroscopy. Buffer was exchanged several times to avoid unbound Cy5 labelled target hybrid oligomers in solution.

Preparation of the micro-fluidics chamber

Silicon elastomer and curing agent, (Sylgard 184, Dow Corning, Wiesbaden, Germany) were well mixed in a 10:1 ratio and were degassed twice at 20 mbar. The solution was poured on a silicon wafer with a lithographically prepared positive relief structure consisting of two parallel flow channels separated by 20 μm. The channels were 20 μm high, 100 μm broad, and about 1 cm long as shown in figure S 1. The system was degassed again and then baked at 60 °C for 1 h. When taken off of the silicon wafer, the PDMS elastomer has the negative structure of the flow channels on its lower side. Cannulas (Sterican, 0,80 x 22 mm, Carl Roth, Karlsruhe, Germany) were pierced through the PDMS in order to provide connections from the upper side to all ends of the channels. The lower side of the PDMS flow channels was contacted with the cover glass slips. A pump was connected to the cannulas on the upper side, such that oligomers and rinsing solutions could be pumped through the channels.

Sequences of the oligonucleotides

DNA bases are denoted with A, C, G, T. RNA bases are denoted with rA, rC, rG, rU. (All oligomers were purchased from IBA, Göttingen, Germany.)

thiolated cantilever oligomer:

5' SH- TTTTT CTGCAGGAATTCGATATCAA

thiolated depot oligomer:

5' SH- TTTTT AAGTAGCTATTCGAACTATAGCTTAAGGACGTCAA

thiolated target hybrid oligomer (α -part of the aptamer):

5' rCrCrA rGrGrU rArArC rGrArA rUrGrG rArUrU TAG CTA TTC GAA CTA TAG CTT
AAG GAC GTC T -SH

transfer hybrid oligomer (β -part of the aptamer):

5' GAC GTC CTT AAG CTA TAG TTC GAA TAG CTA rUrUrU rCrCrC rGrArC rUrGrG TTT
GAT ATC GAA TTC CTG CAG

thiolated transfer hybrid oligomer:

5' GAC GTC CTT AAG CTA TAG TTC GAA TAG CTA rUrUrU rCrCrC rGrArC rUrGrG TTT
TTT T -SH

Cy5 labelled target hybrid oligomer:

5' rCrCrA rGrGrU rArArC rGrArA rUrGrG rArUrU TAG CTA TTC GAA CTA TAG CTT
AAG GAC GTC T -Cy5

Atto647N labelled transfer oligomer:

5' Atto647N-

TTTGACGTCCTTAAGCTATAGTTTCGAATAGCTACTTTTTGATATCGAATTCCTGCAGT

Dissociation Constant of the the split Aptamer

In order to determine the K_d , the fluorescence of a constant amount (87 nM) of assembled aptamer at variable amounts of Malachite Green was measured with a fluorescence spectrometer (Fluoromax-3, JY Horiba, New Jersey, USA). The data is shown in figure S 2. The fit was performed with the function

$$f(MG_{tot}) = F_0 + (F_{max} - F_0) \cdot \frac{A_{tot} + MG_{tot} + K_d - \sqrt{(A_{tot} + MG_{tot} + K_d)^2 - 4A_{tot}MG_{tot}}}{2A_{tot}} \quad (\text{eq. S1})$$

with F_0 the measured offset, F_{max} the maximum fluorescence, A_{tot} the concentration of the assembled aptamer, MG_{tot} the concentration of Malachite Green. This dependency follows directly from the law of mass action and the linear dependence of the overall fluorescence on the fractions of bound and unbound malachite green dye. K_d was determined to be 107 ± 9 nM. This value compares to the K_d of the unsplit Malachite Green Aptamer of 117 nM⁵.

Fluorescence Enhancement Properties

For the determination of the enhancement of quantum efficiency the fluorescence of 400 nM malachite green was measured alone and in presence of 200 nM α -part, β -part and both parts of the split aptamer hybridized in a fluorescence spectrometer. The results are shown in figure S 3,

S 4 and S 5. The measurement was performed in a 100 mM phosphate buffer, pH 5.5, 140 mM NaCl, 5 mM MgCl₂.

It follows from the law of mass action, that the concentration of aptamer bound malachite green is

$$[MGA] = \frac{[MG] + [A] + K_d - \sqrt{([MG] + [A] + K_d)^2 - 4[MG][A]}}{2} \quad (\text{eq. S2})$$

The fluorescence output of the pure malachite green measurement is

$$F_{MG} = f_{spectr} A Q_1 [MG] \quad (\text{eq. S3}) \quad \text{and} \quad F_{Apt} = f_{spectr} A (Q_1 ([MG] - [MGA]) + Q_2 [MGA]) \quad (\text{eq. S4})$$

fluorescence output for the measurement with both parts of the split aptamer and malachite green. K_d is the dissociation constant, f_{spectr} is a spectrometer specific constant, A the absorption of malachite green is approximately independent of the bound or unbound state, [A], [MG], and [MGA] are the concentrations of assembled aptamer, malachite green and malachite green-aptamer complex, and Q₁, Q₂ are the quantum efficiencies of unbound and bound malachite green, respectively. From this follows immediately that the enhancement of quantum efficiency is

$$\frac{Q_2}{Q_1} = \frac{\frac{F_{Apt}}{F_{MG}} + \frac{[MGA]}{[MG]} - 1}{\frac{[MGA]}{[MG]}} \quad (\text{eq. S5})$$

The enhancement factor was here determined to be 1769±74, with K_d=107±9 nM,

$$F_{Apt}/F_{MG}=747±15, [MG]=1000±10 \text{ nM}, [MGA]=500±5 \text{ nM}.$$

The fluorescence of either 500 nM either α-part or β-part of the split aptamer with 1 μM malachite green can directly be compared to the fluorescence of 1 μM malachite green only. It turns out that fluorescence is enhanced by around a factor 3 if either α- or β-part of the split aptamer are present.

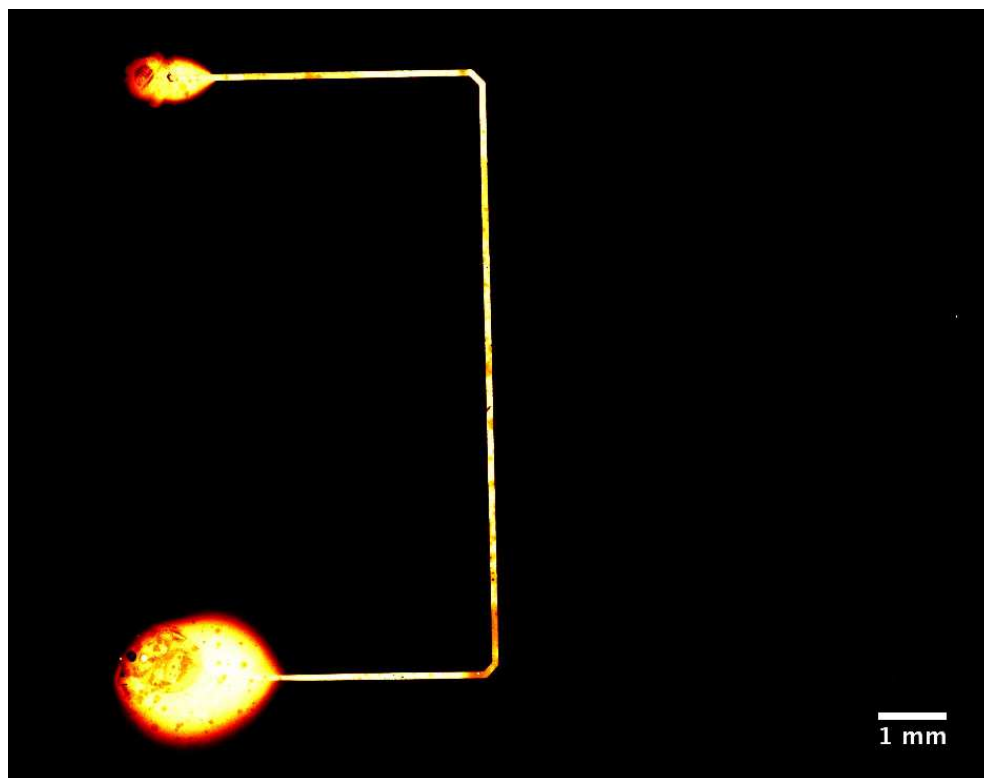
Single-Molecule Fluorescence of Assembled Aptamers

β -strands were covalently bound to the surface as described above. In a very dilute manner Cy5 labeled α -strands were then hybridized. In a 100 mM phosphate buffer, pH 5.5, 140 mM NaCl, 5mM MgCl₂ fluorescence of Cy5 was first recorded by TIRF microscopy until all Cy5 molecules were bleached. The buffer was then exchanged for a 100 mM phosphate buffer, pH 5.5, 140 mM NaCl, 5mM MgCl₂ containing 50 nM or 100 nM malachite green. Next fluorescence of malachite green was recorded by TIRF microscopy. In ImageJ Cy5 fluorescence was averaged, and a standard deviation image of the malachite green fluorescence was calculated. Cy5 fluorescence was displayed with a red color look up table and malachite green fluorescence with a green one. The two images were summed up in ImageJ, such that colocalized spots could be identified (figure S 6). A fraction of red-only and green only spots was also observed. Red-only spots can for example occur, if the surrounding of the aptamer is perturbed in such a way, that binding pockets cannot form or are not accessible. They occur also, if the contribution of the malachite green fluorescence to the overlaid standard deviation image is not exceeding the noise level. E.g. such behavior may be induced by local impurities of/on the surface. Green-only spots occur more often and may indicate, that at these locations malachite green molecules attach non-specifically in such a way, that the phenyl rings loose their rotational degrees of freedom. Here again, local impurities may play a role. Incomplete labeling of the α -strand with Cy5 may also result in a green-only detection. Displacement of the images caused by thermal drift and movements of the instrument when the buffer is exchanged, occur for all functional aptamers in the same direction. Images can after superresolution localization of malachite green and Cy5 be shifted for correction. Colocalized spots that show a displacement in a different direction were not taken into account. 4x4 pixel regions of interest were created for identified spots and z-axis

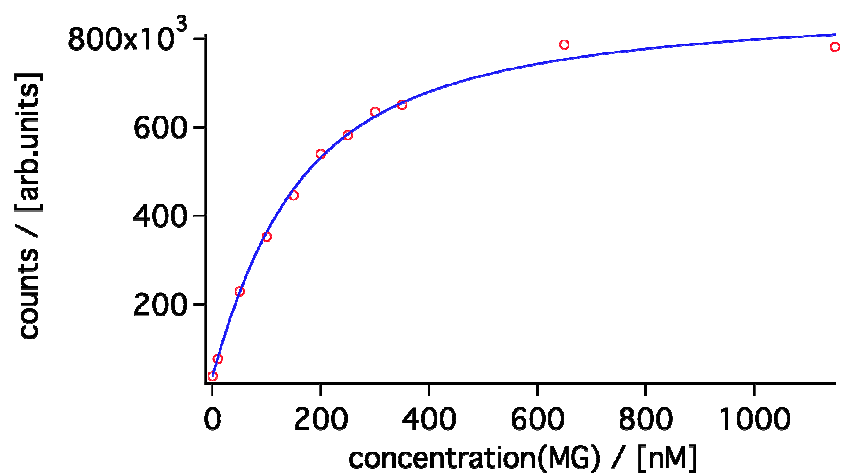
profiles were calculated with ImageJ. Data was then imported into IGOR for further evaluation. The Cy5 fluorescence timetraces were background corrected because some background bleaching was overlaying. The background average value after bleaching was then added as an offset value to the fluorescence timetraces.

Single-Molecule Localization with Nanometer Accuracy

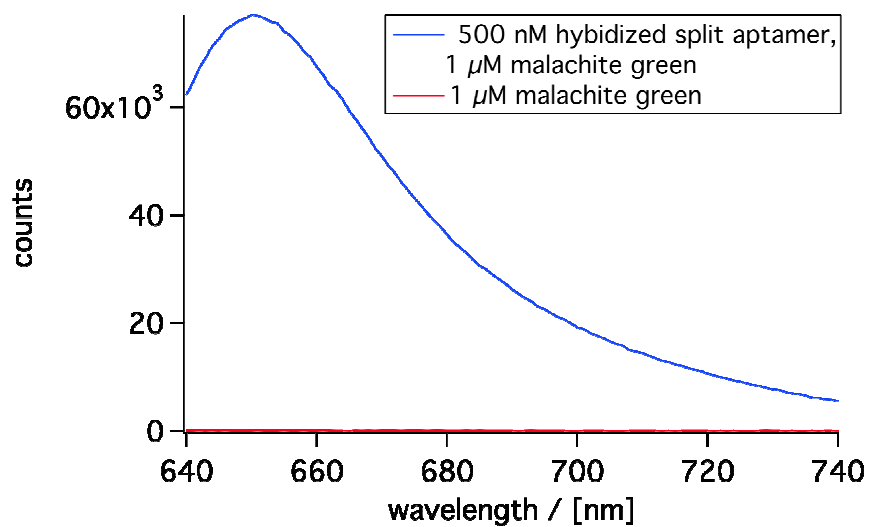
The diffraction limited single molecule fluorescence distribution was taken in TIRF microscopy as described above. Fluorescence of Cy5 and the single aptamer-bound malachite green fluorescence events were averaged in ImageJ. Average images were then imported into IGOR for further calculations. The center of the fluorescence distribution was determined in IGOR by fitting a 2D gaussian to the distribution. A result is shown in figure S 7. Thermal drift on the order of 10 nm causes, that fluorescence events do not overlay exactly. Fitting errors are below 12 nm.



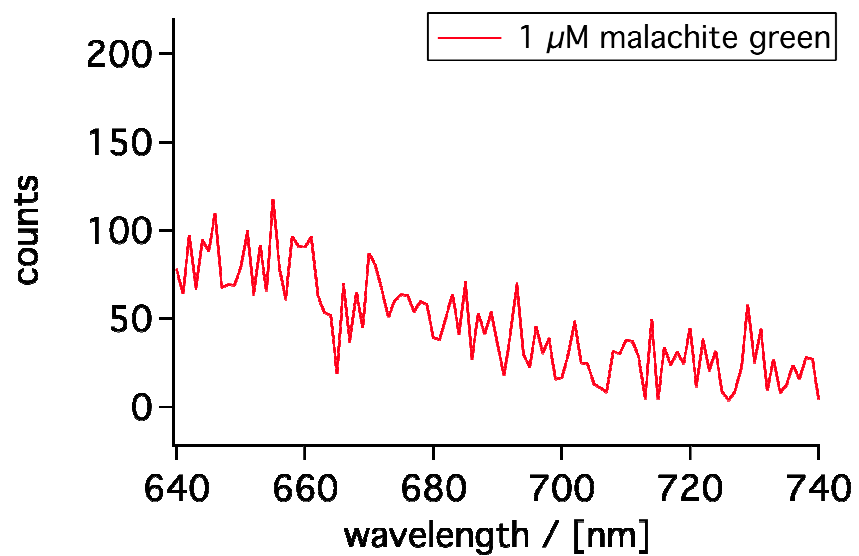
S 1. In a PDMS flow chamber a glass surface was functionalized in a depot region with thiolated depot oligomers. A dye labelled Transfer oligomer was then hybridized to the depot oligomers. The target region on the right side is functionalized with a thiolated target oligomer only. It cannot be seen in fluorescence microscopy. The channel length is about 1 cm, the width 100 μm .



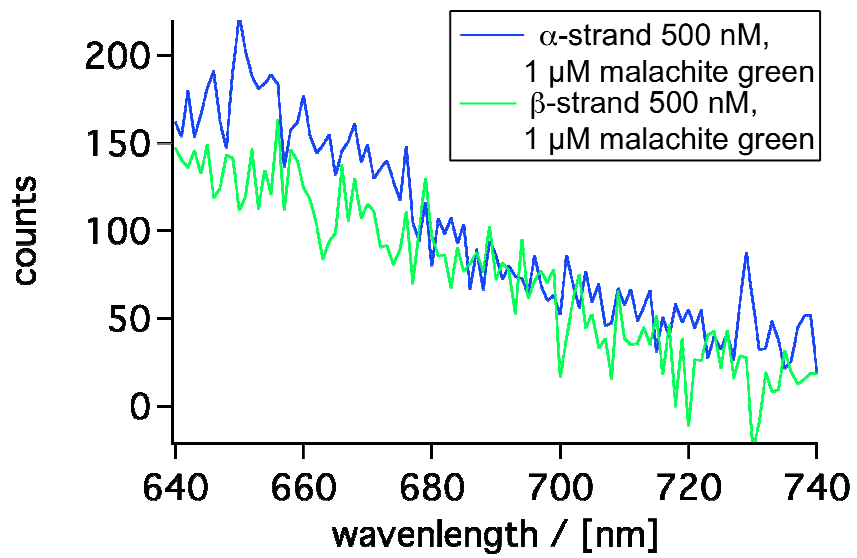
S 2. For the determination of the dissociation constant the fluorescence of aptamer bound malachite green was measured for different malachite green concentrations. The dissociation constant was determined to be 107 ± 9 nM.



S 3. The combined split aptamer units enhance the quantum yield of malachite green by a factor of almost 1800 (blue curve). A detailed graph of the fluorescence of 1 μ M malachite green only (red curve) is given in figure S 4.

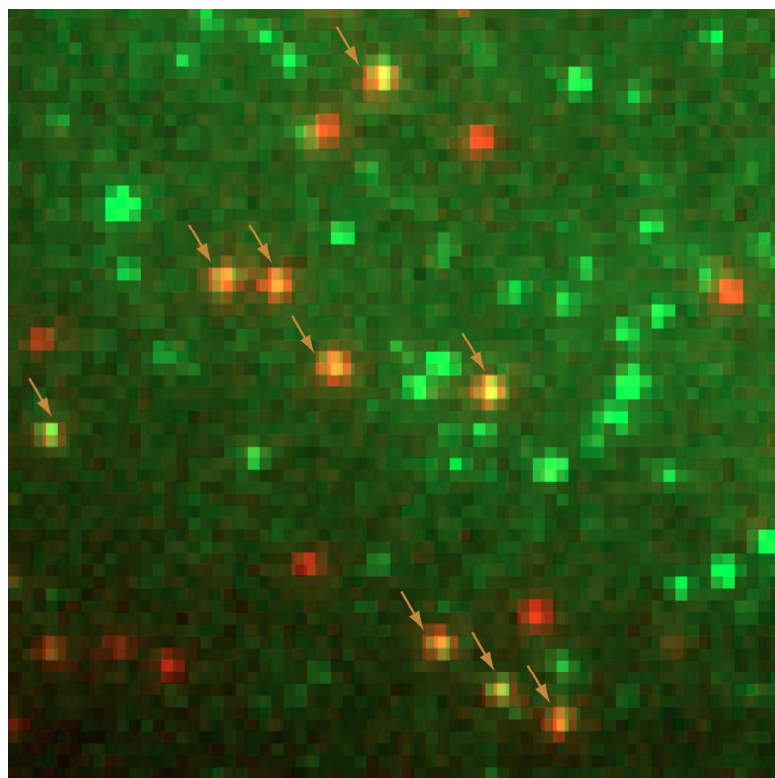


S 4. Fluorescence of 1 μM MG is depicted in this graph. It is extremely weak compared to the fluorescence of malachite green bound by the assembled aptamer.

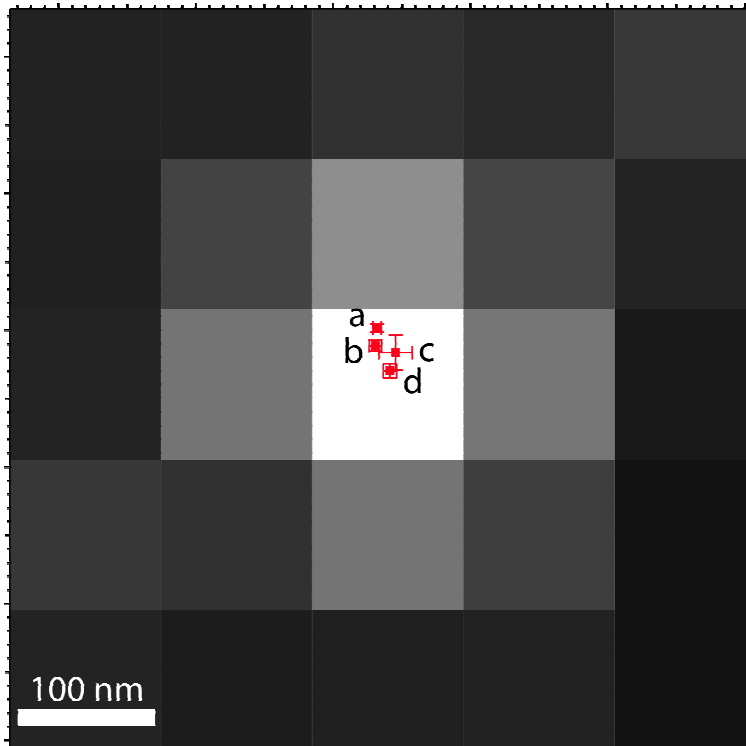


S 5. Fluorescence either of 500 nM α -strand (blue) or β -strand (green) is shown in this graph.

Fluorescence of 1 μ M malachite green is enhanced by only around a factor 3.



S 6. For the identification of individual functional aptamers, an averaged image of the Cy5 fluorescence (red) and an image of the malachite green fluorescence (green) were corrected for drift displacement and overlaid.



S 7. The positions of the Cy5 label (a), and the malachite green fluorescence bursts (b, c, and d in temporal order) were determined by fitting gaussians to the diffraction limited spots. The diffraction limited fluorescent pattern depicted in this graph is that of the malachite green fluorescence burst of (d). Error bars represent the fitting errors. Deviations from the original Cy5 position are on the order of 10 nm and can be assigned to thermal drift.

References:

- 1) Gump, H., Stahl, S.W., Strackharn, M., Puchner, E.M. & Gaub, H.E. Ultrastable combined atomic force and total internal reflection fluorescence microscope [corrected]. *The Review of scientific instruments* **80**, 063704 (2009).
- 2) Florin, E. Sensing specific molecular interactions with the atomic force microscope. *Biosensors and Bioelectronics* **10**, 895-901 (1995).
- 3) Butt, H.J. & Jaschke, M. *Nanotechnology* **6**, 1-7 (1995).
- 4) Zimmermann, J.L., Nicolaus, T., Neuert, G. & Blank, K. Thiol-based, site-specific and covalent immobilization of biomolecules for single-molecule experiments. *Nature protocols* **5**, 975-85 (2010).
- 5) Babendure, J.R., Adams, S.R. & Tsien, R.Y. Aptamers switch on fluorescence of triphenylmethane dyes. *Journal of the American Chemical Society* **125**, 14716-7 (2003).